Biomaterials 31 (2010) 810–817

Contents lists available at ScienceDirect

Biomaterials

journal homepage: www.elsevier.com/locate/biomaterials

Polyketal microparticles for therapeutic delivery to the lung

Vincent F. Fiore [a], Megan C. Lofton [a], Susanne Roser-Page [c], Stephen C. Yang [a], Jesse Roman [c], Niren Murthy [a,b], Thomas H. Barker [a,b,c,*]

[a] The Wallace H. Coulter Department of Biomedical Engineering at Georgia Institute of Technology and Emory University, 313 Ferst Drive, Suite 2108, Atlanta, GA 30332-0535, USA
[b] The Center for Drug Design, Development, and Delivery, Georgia Institute of Technology, Atlanta, GA 30332, USA
[c] Division of Pulmonary, Allergy, and Critical Care Medicine, Department of Medicine, Emory School of Medicine, Atlanta, GA 30322, USA

ARTICLE INFO

Article history:
Received 29 July 2009
Accepted 29 September 2009
Available online 20 October 2009

Keywords:
Biocompatibility
Drug delivery
Fibrosis
Lung
Microsphere
Superoxide

ABSTRACT

Inflammation in the setting of interstitial lung disease (ILD) occurs in the distal alveolar spaces of the lung, which presents significant challenges for therapeutic delivery. The development of aerosolizable microparticles from non-immunogenic polymers is needed to enable the clinical translation of numerous experimental therapeutics that require localization to the deep lung and repeated delivery for optimal efficacy. Polyketals (PK), a family of polymers, have several unique properties that make them ideal for lung delivery, specifically their hydrolysis into non-acidic, membrane-permeable compounds and their capacity to form microparticles with the aerodynamic properties needed for aerosolization. In this study, we tested the lung biocompatibility of microparticles created from a polyketal polymer, termed PK3, following intratracheal instillation in comparison to commonly used PLGA microparticles. We furthermore tested the initial efficacy of PK3 microparticles to encapsulate and effectively deliver active superoxide dismutase (SOD), a free radical scavenging enzyme, in a model of lung fibrosis. Our findings indicate that PK3 microparticles display no detectable level of alveolar or airway inflammation, whereas PLGA induced a small inflammatory response. Furthermore, SOD-loaded into PK3 microparticles maintained its activity upon release and, when delivered via PK3 microparticles, inhibited the extent of lung fibrosis.

1. Introduction

There are a number of diseases characterized by fibrotic remodeling of the lung including idiopathic pulmonary fibrosis (IPF), asbestosis, and cryptogenic organizing pneumonia (COP). Prominent features of these pulmonary fibrotic disorders are excessive fibroblast proliferation and collagen deposition in the lung parenchyma following some type of lung injury. Although most are rare, these disorders usually have a dismal prognosis and a high mortality rate. IPF, characterized histologically by the lesion termed usual interstitial pneumonitis, has an annual death rate higher than that of Alzheimer's disease, and about half that of HIV infection [1,2]. Other diverse disorders, such as the rheumatic diseases, bronchopulmonary dysplasia in premature infants, and occupational exposures, can show prominent fibrotic changes in the lung. Taken together, these disorders, known as interstitial lung diseases (ILD), are a significant cause of morbidity and mortality. What is known of the pathogenesis of pulmonary fibrotic diseases is complex, involving the interplay of genetic predisposition, possible environmental factors, activation of parenchymal cells and immune effector cells, and regulation of a staggering number of inflammatory mediators and matrix components at the local tissue level [3,4]. Antifibrotic therapy to date has consisted of systemic corticosteroids and other immunosuppressive regimens that are fraught with debilitating and sometimes fatal side effects. These regimens do not treat the underlying pathology and thus often have little to no effect on the dismal prognosis, leading some to question their clinical use [5]. Both the organotypic distribution, specifically the distal airways and alveoli deep in the tissue, and the inherent chronic inflammatory origins of these disorders have presented significant challenges with respect to therapeutic delivery directly to the lung. Biomaterials with extraordinary biocompatibility that can be formulated into aerosolizable microparticles are needed for pulmonary delivery to treat both acute and chronic inflammatory and fibrotic lung disorders.

Microparticles formulated from polymeric biomaterials have been heavily investigated for the systemic delivery of peptides and proteins [6,7]. Microparticles 1–3 μm diameter in size, or porous particles 10–20 μm in diameter have the physical properties needed

* Corresponding author. The Wallace H. Coulter Department of Biomedical Engineering at Georgia Institute of Technology and Emory University, 313 Ferst Drive, Suite 2108, Atlanta, GA 30332-0535, USA. Tel. +1 404 385 5039; fax: +1 404 894 4243.
E-mail address: thomas.barker@bme.gatech.edu (T.H. Barker).

0142-9612/$ – see front matter © 2009 Elsevier Ltd. All rights reserved.
doi:10.1016/j.biomaterials.2009.09.100

for inhalation from a dry powder spinhaler and deposition into the alveolar region of the lung [8–10]. In contrast, generating micron sized powders from peptides, proteins, or small molecules, such as mannitol or sucrose, has been challenging, and for this reason, microparticles formulated from polymers are increasingly being considered for protein and peptide delivery [11]. Both natural and synthetic polymers, such as hydroxypropyl cellulose, chitosan, gelatin, and poly(lactic-*co*-glycolic acid) (PLGA), have been studied as potential vehicles for inhalable protein delivery. Sivadas et al. have recently performed a comparative study of such polymers [6]. Inhalable polymeric microparticles can also be advantageously used as an inhalable controlled-release delivery system, maintaining a high concentration of therapeutic within the lung for an extended period of time.

PLGA has been extensively investigated for the inhaled delivery of therapeutics, however its acidic degradation products and slow hydrolysis rates have thus far limited its clinical use. Previous studies report that an intratracheal dose of 1 mg of PLGA microparticles in a rodent model results in a large recruitment of white blood cells to the lungs, indicative of an inflammatory response [12]. Within 24 h of injection, PLGA treated lungs contained $\sim 10^5$ macrophages/mL of bronchoalveolar lavage (BAL) fluid, whereas controls contained only 10^4 macrophages/mL BAL fluid. Similarly, neutrophil influx is dramatically increased in PLGA treated rodents. The white blood cell influx cleared within 10 days, although PLGA microparticles resided in the lung tissue for approximately 80 days with an estimated half-life of 40 days. The acidic degradation products of PLGA can also be problematic for the delivery of numerous peptides and proteins [13]. The pH within PLGA can reach values of 2–3, and this low pH can catalyze various hydrolysis reactions in peptides and proteins.

In contrast to PLGA, polyketals, which degrade into neutral compounds, should not elicit the inflammation associated with polyester based materials. The polyketal termed PK3, which has been recently described, is a copolymer of 1,4-cyclohexanedimethanol and 1,5-pentanediol that degrades into neutral byproducts of diols and acetone [14]. Specifically, PK3 degrades into its comprising diols (1,4-cyclohexanedimethanol: $LD_{50} = 3{,}200$ mg/kg (Rat – oral); 1,5-pentanediol: $LD_{50} = 10{,}000$ mg/kg (Rat – oral)) and acetone ($LD_{50} = 5{,}800$ mg/kg (Rat – oral)) which have extremely low toxicity profiles. Furthermore, PK3 undergoes acid-catalyzed hydrolysis, exhibiting a half-life of 1.8 days at a pH of 4.5 versus 39 days at pH = 7.4. This enables accelerated delivery of the microparticle's contents within the lowered pH of the phagolysosome.

In this study, a potential therapeutic, superoxide dismutase (SOD), was encapsulated and delivered using PK3. SOD is the human body's endogenous antioxidant against superoxide (O_2^-), a free radical species and known inducer of oxidative stress. SOD catalyzes the dismutation of superoxide into molecular oxygen (O_2) and hydrogen peroxide (H_2O_2), which is further detoxified into water by catalase, glutaredoxins (e.g. glutathione peroxidase), thioredoxins, or peroxiredoxins [15]. A depletion of SOD and subsequent induction of reactive oxygen species (ROS) and oxidative stress has been implicated in the progression of pulmonary disorders including IPF [16]. Specifically, it has been shown that extracellular SOD-null mice have increased susceptibility to bleomycin-induced fibrosis, and that targeted overexpression of the enzyme attenuates fibrosis [17,18]. SOD also has been shown to be severely depleted from fibrotic regions of the lung during disease, both in the rodent model and human patient condition [19–21]. Therefore, delivery of exogenous SOD has been hypothesized to protect the lung against oxidative injury and has been shown to attenuate the effects of bleomycin-induced pulmonary fibrosis [22]. Various strategies to deliver SOD to the lungs have been employed, such as PEGylation of SOD to improve circulation half-life, or liposome-mediated delivery of the enzyme [23,24]. Here, we describe the delivery of SOD locally to the lung and with a polymer vehicle designed to illicit no inflammatory response and capable of translation to a dry particle inhaler.

2. Materials and methods

2.1. Materials

Poly(lactic-co-glycolic acid) (PLGA, 50:50) was purchased from Polysciences, Inc. (Warrington, PA), SOD determination kit from Fluka (Buchs, Switzerland), BCA Protein Assay from Pierce (Rockford, IL), Hematoxylin and Eosin stain from Richard–Allan Scientific (Kalamazoo, MI), and polystyrene standards from Polymer Laboratories (Amherst, MA). All other chemicals, including superoxide dismutase (SOD), were purchased from Sigma (St. Louis, MO).

2.2. PK3 synthesis

PK3 was synthesized via an acetal exchange reaction between 1,4-cyclohexanedimethanol (1.04 g, 7.25 mmol) and 1,5-pentanediol (0.11 g, 1.08 mmol) as described previously [25]. Diols were dissolved in 20 mL of distilled benzene and kept at 100 °C. Re-crystallized *p*-toluenesulfonic acid (5.5 mg, 0.029 mmol), dissolved in ethyl acetate (500 μL), was added to the benzene solution. Ethyl acetate was distilled off, and distilled 2,2-dimethoxypropane (0.86 g, 8.3 mmol) was added to initiate the reaction. Additional doses of 2,2-dimethoxypropane and benzene were subsequently added to the reaction, every hour for six hours, via a metering funnel, to compensate for 2,2-dimethoxypropane and benzene that had been distilled off. After 24 h, the reaction was stopped by adding triethylamine (100 μL). PK3 was isolated by precipitation into cold hexanes and analyzed by ^{1}H NMR and GPC. In general PK3 batches had a number average molecular weight between 3000 and 4000 Da. ^{1}H NMR spectra were obtained from a Varian Mercury VX 400 MHz NMR spectrometer (Palo Alto, CA) using $CDCl_3$ as the solvent. ^{1}H NMR (400 MHz, $CDCl_3$, δ): 3.4–3.18 (m, 4H, CH_2), 1.64 (s, 1.7H, CH), 1.85–0.93 (m, 8.2H, CH_2).

2.3. Microparticle fabrication

Microparticles were produced by standard emulsion techniques. Empty particle synthesis consisted of a single emulsion of 5% polyvinyl alcohol (PVA) solution (50 μL) homogenized in 500 μL of 80 mg/mL PK3 or PLGA in dichloromethane (DCM) (6500 RPM). In the case of loaded particles, superoxide dismutase (Cu, Zn SOD) was encapsulated in PK3 via a solid-in-oil-in-water double emulsion (s/o/w) procedure. SOD was complexed with polyethylene glycol (PEG) to shield it from DCM in the primary emulsion, improving enzyme activity encapsulated in the microparticles [26]. SOD and PEG were dissolved in DIH_2O (deionized H_2O) at a 1:1 ratio and then snap frozen and lyophilized at 0.1 mBar overnight. The SOD-PEG mixture (5 mg) was added to the DCM-polymer solution and sonicated using a Branson S-250A sonifier (Danbury, CT) at 12 watt energy output for 30 s to yield the solid-in-oil primary emulsion. Five percent buffered (pH 6.8) PVA solution was added to the primary emulsion and homogenized (Fisher Scientific, Waltham, MA) at 6500 RPM for 1 min, yielding the secondary emulsion. The emulsion was cycled between low and high pressures using a Buchi R-210 rotary vaporizer (Flawil, Switzerland) to remove DCM. The particles were then washed (2×) in DIH_2O deionized water, after which the suspended particles were frozen and lyophilized at 0.1 mBar overnight.

2.4. Microparticle characterization

2.4.1. Dynamic light scattering (DLS)

Standard dynamic light scattering was performed using a Brookhaven 90Plus particle sizer (Brookhaven Instruments Corp., Holtsville, NY) to characterize microparticle size distributions. Particles were analyzed during the synthesis process after solvent removal, but prior to particle washing. Particle suspension measurements were taken over 1 min. at 25 °C to determine the particle effective diameter and particle size distributions.

2.4.2. Scanning electron microscopy (SEM)

High-resolution images (3000×) were obtained of the lyophilized particles using a Hitachi Leo 1530 SEM (Tokyo, Japan). Samples were prepared by affixing double-sided carbon tape to 12 mm pin type SEM mounts. Microparticles were gently spread across the top of the carbon tape. Adhered particles were gold coated using a sputter-coater and imaged to visualize particle morphology.

2.4.3. SOD encapsulation efficiency and activity assay

A 2 mg sample of the SOD microparticles was placed in DCM in order to dissolve the PK3 polymer. DCM was allowed to evaporate using an oil bath at 60 °C followed by addition of DIH_2O to solubilize the protein encapsulated within the microparticles. SOD activity was then determined using the SOD determination kit according to the manufacturer's instructions and compared with prepared standards. Results from the SOD activity assay were compared to a BCA assay for total protein content to determine the percentage of active protein.

Encapsulation efficiency and enzyme activity (% total) were calculated according to the following:

$$\text{Encapsulation efficiency } (\%) = \frac{\text{encapsulated protein}}{\text{total protein used in formulation}}$$

$$\text{Enzyme activity } (\%) = \text{active enzyme/total encapsulated protein}$$

2.5. Lung biocompatibility of microparticles

2.5.1. Intratracheal administration of particles

Particles (PK3 and PLGA) of equivalent physical characteristics were injected intratracheally into C57BL/6 male mice (20–25 g) to assess microparticle biocompatibility *in vivo*. All mice were anesthetized according to IACUC standards by intraperitoneal injection of ketamine/xylazine solution. A small incision was made submandibularly to expose the trachea. Using a sterile syringe, the trachea was punctured and particle–saline suspensions injected. Experimental groups included particle suspensions composed of 1.5 mg of PK3 and 1.5 mg of PLGA in 50 μL sterile saline. Control groups included bleomycin, vehicle, and non-treated mice. After injections, mice were sutured and allowed to recover. For the experimental and bleomycin groups, mice were sacrificed at days 1, 4, and 7. For the vehicle control, mice were sacrificed at day 5, and the untreated control group at day 0. Immediately following sacrifice, a bronchoalveolar lavage (BAL) was performed and the lung harvested.

2.5.2. Bronchoalveolar lavage (BAL) and airway inflammatory cell analysis. Following euthanasia, the trachea was exposed with a submandibular incision. Sterile PBS (1.5 ml) was injected into the trachea to fill all five lobes of the lung. The BAL was then recovered in the same syringe. Following centrifugation, cell pellets were resuspended in PBS (100 μL) and prepared for staining and quantification by standard cytospin procedures. Using the Cytospin 2 (Shandon Inc., Pittsburgh, PA) cells were centrifuged onto slides at 1500 rpm for 7 min. Samples were fixed and stained using a Lueco Stat kit (Fisher Scientific, Waltham, MA), and a cell count of major inflammatory/immune cells was performed in at least 10 random fields. Average cell numbers (macrophage, neutrophils, and lymphocytes) per field are reported.

2.5.3. Histological analysis. Immediately following the BAL, lungs were harvested from each time point and experimental/control group. The trachea was cannulated and left intact during the removal of the lungs from the body. Using the cannula, the lungs were inflated with 10% buffered formalin and then stored in 15 ml of 10% buffered formalin until paraffin embedding. Lungs were embedded in paraffin, sectioned, and stained with hematoxylin and eosin (H&E) for imaging.

2.6. PK3-SOD microparticles in bleomycin-induced lung fibrosis

2.6.1. Bleomycin model of lung fibrosis

Intratracheal injection of bleomycin is the best characterized and most used model of pulmonary fibrosis in mice. Mice were anesthetized and the trachea exposed as done previously [27,28]. Bleomycin in a sterile saline solution was administered at a dose of 3.2 U bleomycin/kg body weight (50 μL). Particles of SOD-PK3, PK3, or PLGA were co-administered with bleomycin at a dose of 100 μg (groups of $n = 5$). Groups of PBS (vehicle control), bleomycin only (positive control) and SOD alone were also included as controls. Mice were euthanized at 14 days and lungs were harvested.

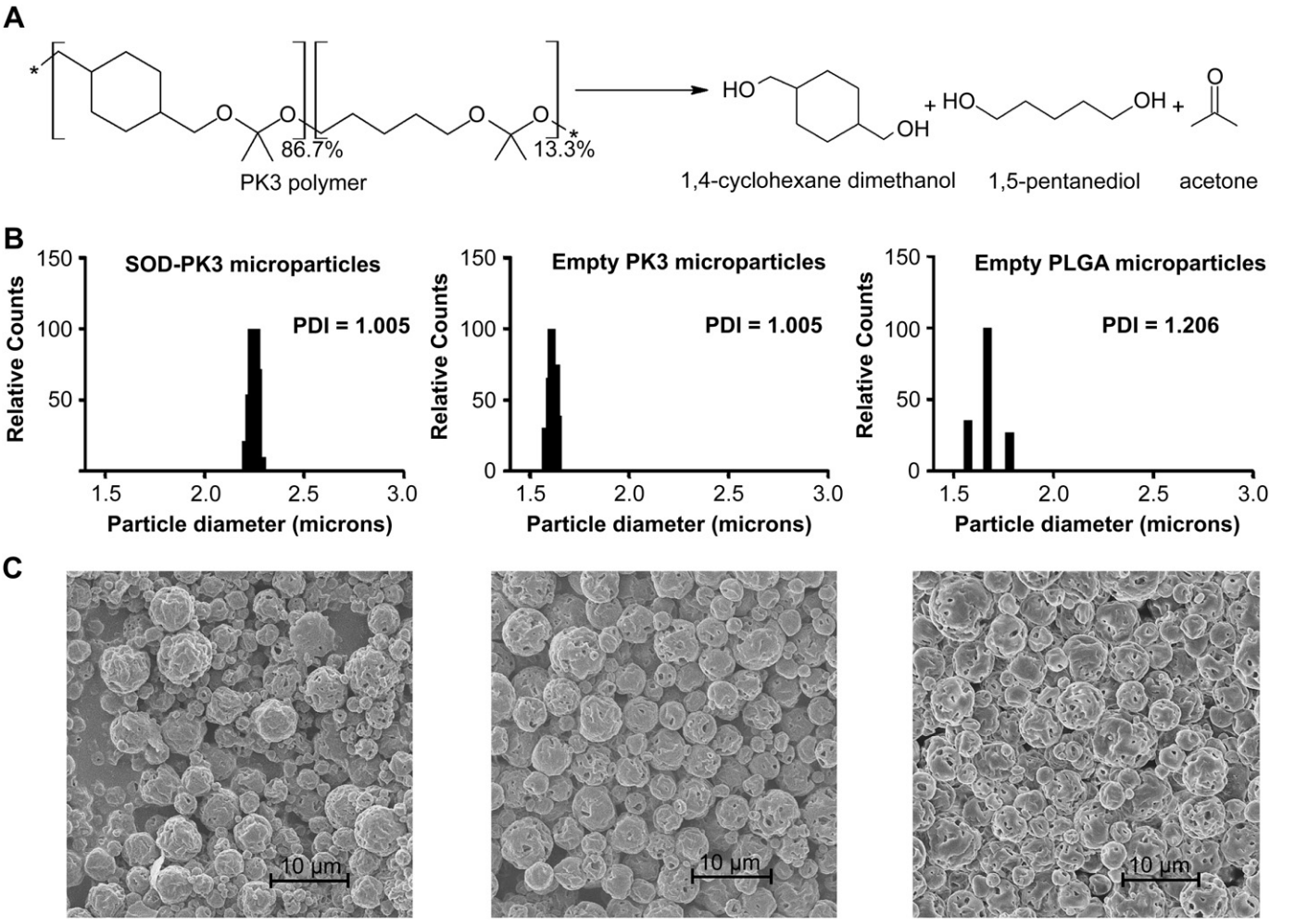

Fig. 1. Microparticle characterization. (A) Structure and hydrolysis schematic of polyketal, PK3. (B) Freshly synthesized SOD-PK3, empty PK3, and empty PLGA microparticles were analyzed by dynamic light scattering (DLS) to determine the average size and particle size distribution. (C) Microparticles were subsequently visualized by scanning electron microscope (SEM) to qualitatively assess their size, polydispersity, shape and porosity.

2.6.2. Lung histology and morphometric analysis of fibrosis

Paraffin embedding, sectioning, and H&E staining were performed as previously described. H&E stained sections were imaged and analyzed for mean alveolar wall fraction (MAWF). The wall thickness of individual alveoli increases due to fibrosis (cellular invasion of interstitium and ECM production) and interstitial edema [29]. To quantify the overall thickening of the alveolar wall due to fibrosis, the alveolar wall area fraction was calculated. MAWF was quantified using the NIS-elements image analysis software. Using a 10× objective lens, 10 randomly selected fields lacking visible blood vessels or airways were analyzed and values averaged per sample. To calculate the alveolar wall area fraction, a field of interest measuring 275 × 205 μm was analyzed by dividing the amount of stained tissue by the constant field of interest area [29].

2.6.3. Hydroxyproline analysis

The left lung lobe was dissected at the time of lung harvesting, weighed, and homogenized at 24000 RPM. Tissue samples were hydrolyzed in 6 N HCl for 16 h at 110 °C. The hydrolysate was buffered with an equal volume of 6 N NaOH, filtered, and a measured aliquot removed. Hydroxyproline was converted to pyrrole-2-carboxylic acid by oxidizing the samples with 0.2 mol/L chloramine-T. After 20 min, Ehrlich's reagent (*p*-diethylaminobenzaldehyde) was added and optical density read by spectrophotometry at 557 nm. Standard 2-hydoxy-L-proline (Sigma Chemical Co.) was used to generate a standard curve and values are expressed as μmol of hydroxyproline per lung.

2.7. Statistical methods

All data were expressed as the average with standard error. First, a one-way ANOVA was used to determine statistical difference among the groups, and then Tukey's test was used as a follow-up to compare the means of each group to every other group. Confidence intervals greater than 95% were considered statistically significant. For BAL analysis of cell infiltrate at 1, 4, and 7 days, a two-way ANOVA was used with Bonferroni's post-test at 95% confidence intervals to determine significance between groups.

3. Results

3.1. Size and protein loading of PK3 microparticles

Polyketal and PLGA microparticles fabricated via double emulsion were analyzed for their size characteristics using DLS. All particles used in the study had mean diameters between 1.5 and 2.5 μm (Fig. 1). Particle size distributions had polydispersity index (PDI) values close to 1, indicating highly monodisperse samples (monodisperse; PDI < 1.1). Particle morphology visualized with SEM images indicates that the particle processing techniques employed produce solid, homogeneous spherical particles.

SOD was encapsulated in PK3 polymer microparticles and the encapsulation efficiency and recovered enzyme activity was determined. The encapsulation efficiency was determined to be 9.3% using the solid-in-oil-in-water emulsion. Encapsulated protein was then assayed to ensure its maintenance in the active state. Standard analysis revealed that the enzyme maintained 87.5% of its initial activity (i.e. the activity of the SOD stock) as determined by assays for SOD enzyme activity and total protein content.

3.2. Inflammatory response to PK3 microparticles in the lung

Lung histology was performed to determine the effect of the different polymer microparticles (PK3 and PLGA) on lung architecture and inflammation. Bleomycin, used as the positive control, showed a characteristic increase in inflammation, thickening of

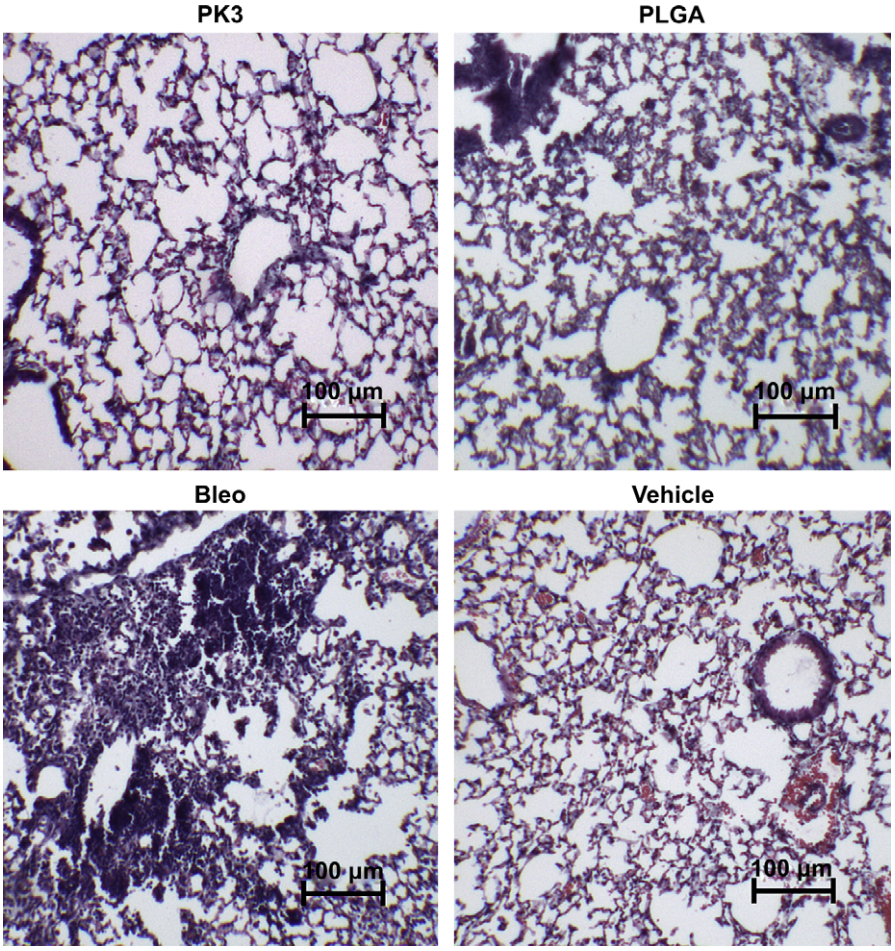

Fig. 2. Histological analysis of lung inflammation. PK3 and PLGA particles were injected intratracheally into mice to determine their specific lung biocompatibility. Bleomycin, a known inducer of acute lung inflammation leading to fibrosis was used as the positive control, and sterile saline ("vehicle") was used as the negative control for lung inflammation in response to fluid instillation. Magnification bars are 100 μm.

alveolar septae, and distortion of normal lung architecture by the presence of pneumonitis. PLGA treated lungs displayed a mild increase in inflammation and increased alveolar wall thickening. PK3 microparticle-treated lungs displayed a phenotype more similar to that of the vehicle control, PBS, and normal lung phenotype with no significant inflammation or alveolar wall thickening (Fig. 2).

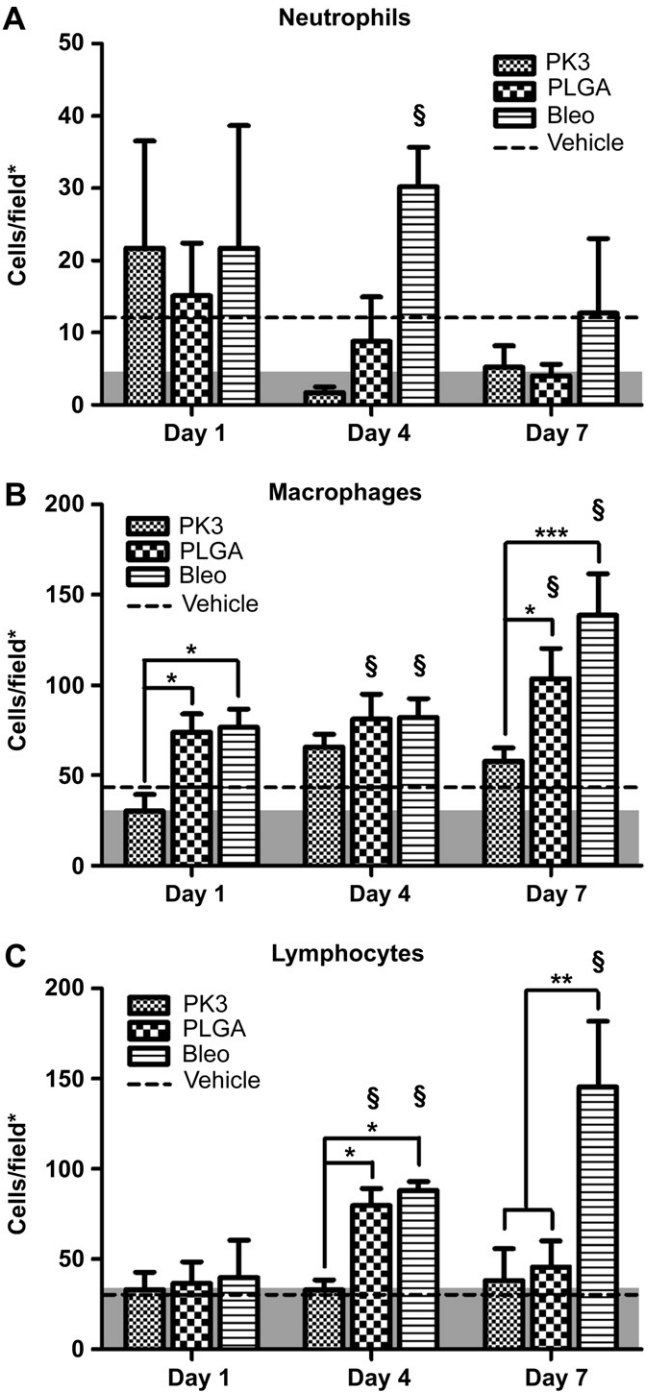

Fig. 3. Quantitative analysis of inflammatory cell infiltration of alveolar space. Bronchoalveolar lavages (BAL) were performed to collect airway and alveolar constituents following treatment with PK3 or PLGA microparticles, bleomycin, or saline. Neutrophils (A), Macrophages (B), and Lymphocytes (C) were quantified by counting in a minimum of 10 random fields (approximately 0.14 mm^2). The horizontal dashed line denotes the vehicle control (saline) level at day 5. The gray region denotes normal (untreated) lung levels. The average cells per field +/− the standard error is reported. $ denotes $p < 0.05$ between the sample group and the vehicle control. * denotes $p < 0.05$ and *** denotes $p < 0.001$ using two-way ANOVA with Bonferroni's post-test between individual groups.

Neutrophil, macrophage, and lymphocyte cell infiltration due to particle instillation was analyzed using BAL fluid collected at various time points (Fig. 3). Neutrophil cell counts (Fig. 3a) revealed an immediate (day 1) increase after solution instillation regardless of the treatment group, including the sterile saline control (dashed line). Neutrophil numbers for both PK3 and PLGA treated lungs were restored to untreated tissue baselines (gray area) at day 4 while the positive control (bleomycin) remained elevated. By day 7 all treatments returned to near baseline levels. Analysis of BAL macrophages (Fig. 3b) at day 1 indicated that the PK3 microparticles ellicit a significantly reduced response than both PLGA and bleomycin control. At day 4, the macrophage levels for all treatments were above the saline control and were not significantly different from each other. However, by day 7, PK3 treated lungs returned to near saline control levels while the macrophage counts of both PLGA and bleomycin continued to increase above day 4 levels and were again statistically greater than both PK3 and saline control treated lungs. Assessment of lymphocyte numbers (Fig. 3c) demonstrated a characteristic "late" response with no significant differences between any of the treatment or control groups, as well as the untreated baseline levels. On day 4, both PLGA and bleomycin treated groups displayed an approximately 2-fold increase in the number of airway lymphocytes that reached significance while PK3 treated group lymphocyte levels remained at saline and baseline levels. By day 7, the number of lymphocytes due to PLGA returned to baseline levels while bleomycin continued to show a characteristic rise toward pulmonary fibrosis. PK3 remained at the saline and baseline levels throughout the experiment.

3.3. *Efficacy of SOD-PK3 microparticles in bleomycin-induced fibrosis*

The effects of PK3 encapsulated-SOD microparticles on pulmonary fibrosis were assessed using biochemical and morphological techniques. H&E stained lung sections (Fig. 4) showed significantly improved lung architecture at 14 days post-bleomycin and particle injection in lungs treated with SOD-PK3 microparticles. The addition of SOD-loaded PK3 microparticles to bleomycin treated lungs resulted in lung architecture similar to normal or vehicle control (PBS) phenotypes. Lungs treated with empty PK3 microparticles and bleomycin display patchy regions of fibrosis and alveolar wall thickening interspersed within regions presenting mostly normal architecture. In contrast, PLGA microparticle-treatment with bleomycin resulted in a typical pulmonary response to bleomycin with significant alveolar wall thickening, cellular infiltration into alveolar spaces, and disruption of alveoli. Finally, lungs treated with soluble SOD at the time of bleomycin instillation present a mostly fibrotic lung with some interspersed regions of aberrant, but not fibrotic, architecture.

Analysis of collagen content based on the assay for hydroxy-L-proline showed a significant increase in collagen over the negative control due to bleomycin administration, as expected (1.5 ± 0.4 versus. 0.8 ± 0.3 μmol/lung)(Fig. 5). None of the test groups (bleomycin plus SOD-PK3, PK3, PLGA, or SOD alone; 1.2 ± 0.3, 1.4 ± 0.4, 1.5 ± 0.3, 1.4 ± 0.3 μmol/lung) demonstrated a significant difference compared to bleomycin treatment only. However, the SOD-PK3 microparticles and free SOD displayed no significant difference with respect to the saline (vehicle) control, whereas significant differences were observed between the PLGA and PK3 microparticle groups and the saline control.

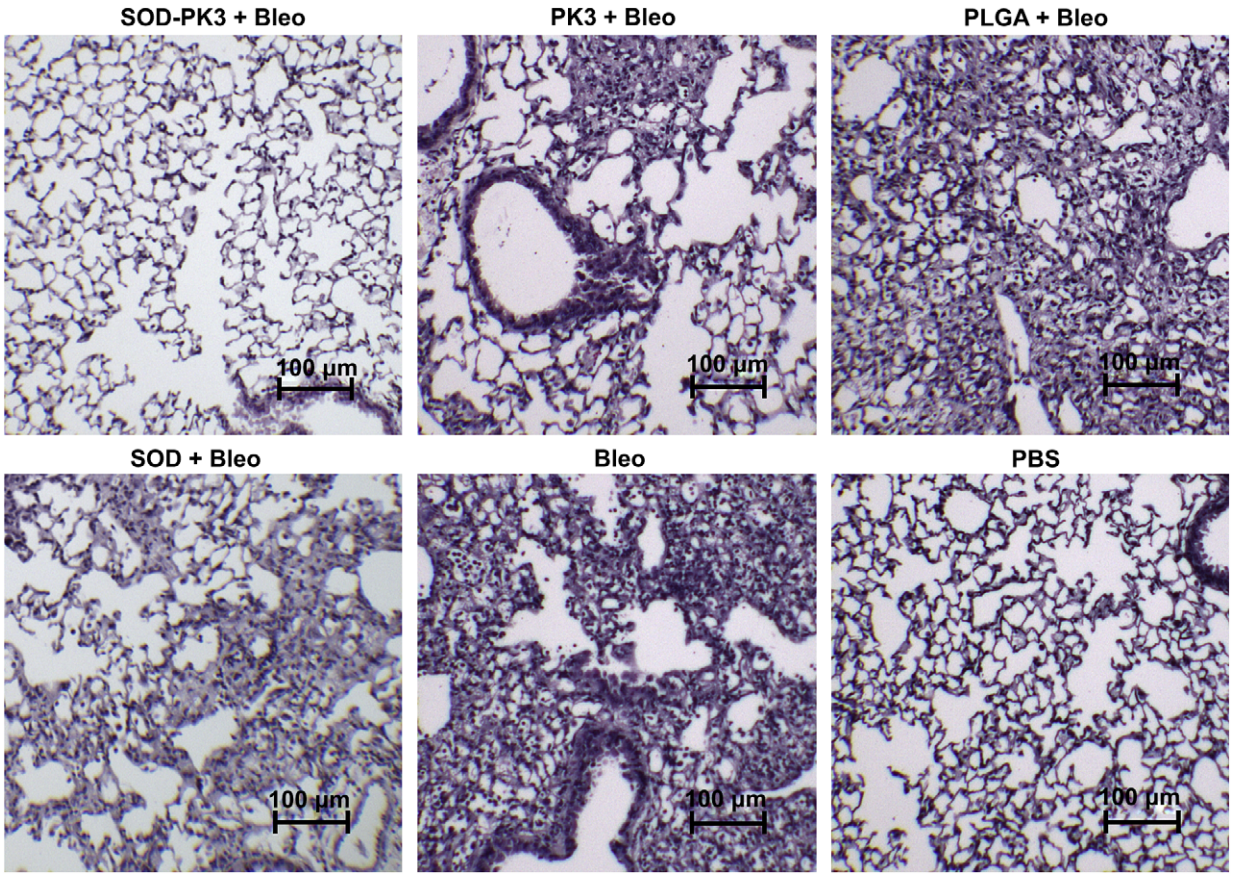

Fig. 4. Histological analysis of bleomycin-induced fibrosis. SOD-loaded PK3 microparticles, empty PK3 microparticles, empty PLGA microparticles, or soluble SOD was co-delivered with the administration of bleomycin to test the initial efficacy of SOD-loaded PK3 microparticles to prevent fibrosis. Bleomycin alone and sterile buffered saline were used as positive and negative controls of fibrosis, respectively. Magnification bars are 100 μm.

H&E stained histological images analyzed for the MAWF were compared among groups, and one-way analysis of variance (ANOVA) determined a significant difference between groups tested. The Tukey post-test determined a significant difference ($p < 0.05$) between the vehicle control (PBS), with an alveolar wall area fraction of $12.9 \pm 0.9\%$, and all other groups except SOD-PK3 ($15.4 \pm 2.6\%$) and empty PK3 ($17.4 \pm 3.9\%$) microparticles. However, no statistical significance was calculated between the loaded particle group and the positive control.

4. Discussion

Lung disease presents significant challenges in therapeutic delivery. Pathological regions in lung diseases are routinely distributed throughout the lung, requiring efficient delivery of the active ingredient to all surfaces. Local delivery is a significant hurdle since the lung has a complicated structure that prevents physical deposition of a product by physicians and surgeons directly onto the affect region(s). However, significant progress has been made on the delivery of inhaled products with the most notable successes being inhaled mists for airway delivery. Interstitial lung diseases are significantly more complicated since the product must be localized to the deep alveolar regions of the lung. Despite efforts to develop nebulization technology that can efficiently produce liquid particles with the correct aerodynamic properties for alveolar delivery, these devices are still cumbersome for individuals to carry and use. Furthermore, the stability of protein and peptide therapeutics due to the aqueous environment and thermal and surface effects during nebulization are limitations. Polymeric biomaterials are a potential solution to some of these pressing issues. Microparticles can be synthesized with architectures that enable aerosolization despite significantly large actual diameters. By engineering porosity into polymeric microparticles, one can create large particles that have the aerodynamics necessary for delivery to the alveoli, yet with a large actual diameter these particles may become trapped in the alveolus, thus delivering their therapeutic cargo. With this delivery philosophy in mind, a significant number of works have demonstrated proof-of-concept with polylactide co-glycolic acid (PLGA) polymeric microparticles.

One potential limitation of PLGA is the biomaterial itself. Although its utility has been demonstrated extensively in animal models of lung delivery, its degradation into acidic byproducts could potentially serve to aggravate the underlying inflammation. Ideally, one would like to construct a microparticle from a polymer that displays similar hydrophobicity as PLGA, so as to enable aerosolization, yet degrades into neutral products so as to avoid perpetuating the underlying pathology. Polyketals may present a possible solution to some problems associated with PLGA delivery to the lung.

Polyketals are a class of polymer that degrade into neutral acetone and diols, and thus may exhibit better biocompatibility in an inflammatory-primed tissue like the lung. We tested the hypothesis that polyketals, specifically PK3, would display better biocompatibility in the lung while enabling the delivery of a test therapeutic, SOD, in a model of lung fibrosis. From our initial studies, we observe that both PLGA and PK3 are extremely non-immunogenic polymers in the mouse lung. Compared to the positive control of bleomycin, both polymers displayed good biocompatibility. However, PK3 microparticles did not display any significant increase

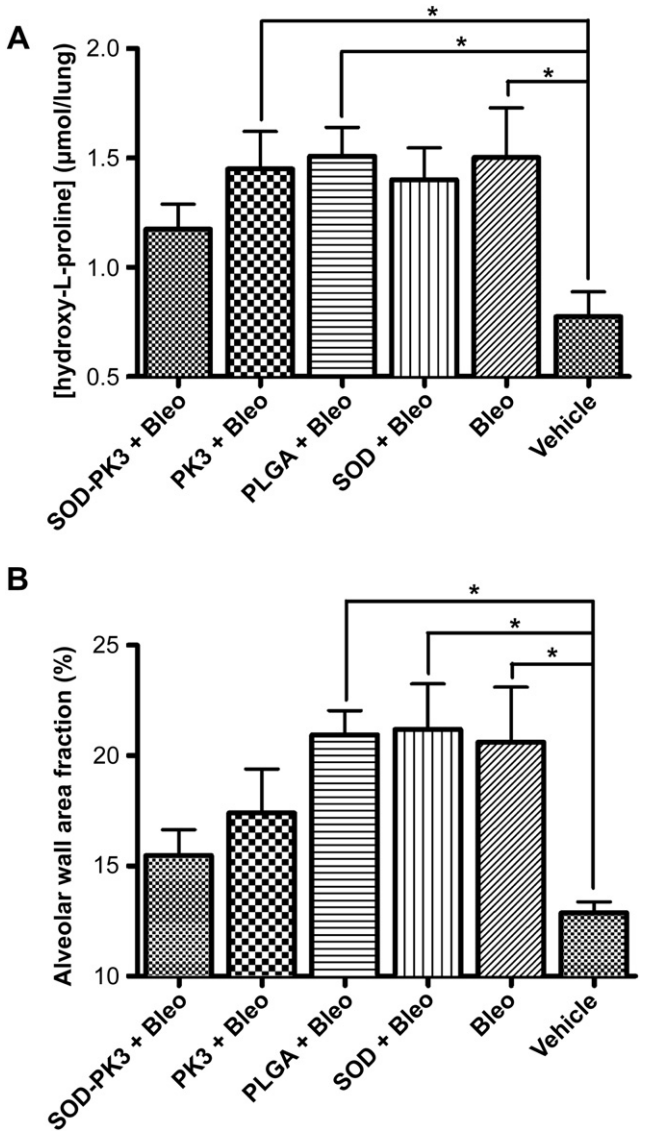

Fig. 5. Quantitative analysis of lung fibrosis. (A) Total hydroxy-L-proline (μmol/mg lung) was quantified on the left lung lobe of experimental groups (SOD-PK3, empty PK3, empty PLGA, soluble SOD, bleomycin only, and vehicle (saline)). (B) Alveolar wall area fraction, a measure of interstitial thickening associated with lung fibrosis, was quantified from images of the histological staining from a minimum of 5 random fields from each sample group. * denotes a statistical significance of $p < 0.05$ using a one-way ANOVA with Tukey's post-test.

in airway inflammation above the saline control, as opposed to PLGA microparticles, which did induce a significant macrophage infiltration starting at day 4 and continuing through day 7 and a transient lymphocyte infiltration at day 4. The extreme biocompatibility of polyketals in the lung may be due to the reported anti-inflammatory activity of its degradation product, acetone [30]. However, further studies would be required to elucidate the mechanism of this PK3 action. Nevertheless, PK3 displays a very attractive biocompatibility profile in the lung and is practically "stealth" in its inflammatory profile.

PK3 microparticles are also efficient delivery vehicles as we achieved nearly a 10% loading efficiency of SOD into microparticles, while maintaining over 87% of the native bioactivity of the protein. In the bleomycin-induced lung fibrosis model, mice given SOD-loaded PK3 microparticles were statistically indistinguishable from the saline control and, while there was no significant difference between these mice and the bleomycin control, these data indicate a significant beneficial effect is attainable with appropriate dosing. Previously published studies displaying near complete attenuation of bleomycin-induced fibrosis using SOD employed dosing of approximately 55 times greater than that of the current study [22]. Surprisingly, empty PK3 microparticles had a slight, but not significant, benefit in the bleomycin-induced lung model as well. Analysis of MAWF in mice treated with empty PK3 microparticles following bleomycin instillation were statistically indistinguishable from the saline control whereas differences between all other control groups (PLGA, soluble SOD, and bleomycin) and the saline control were statistically significant. Again, it is unknown what affect the released acetone from PK3 microparticles has in the lung, but previous reports of an anti-inflammatory activity support our findings that PK3 alone decreases MAWF following bleomycin treatment, a measure of interstitial inflammation, but not hydroxyproline, a measure of collagen deposition.

5. Conclusions

In this study we report significant findings on the lung biocompatibility of polyketal polymers. While additional studies will be necessary to fully realize the use of this class of polymers in lung therapeutic delivery, the data presented here establish the high level of biocompatibility of these polymers and further implicate their purported anti-inflammatory behavior. If borne out in future studies, the anti-inflammatory activity of these biomaterials could have a significant beneficial effect in therapeutic delivery, not only on lung diseases, but potentially any inflammatory disease.

Acknowledgements

Valuable assistance in the acquisition of SEM images was provided by Chen-Yu Kao. Funding was provided by the Wallace H. Coulter Foundation (THB & JRR) and NIH U01 HL80711-01 (NM).

References

[1] Hoyert DL, Kochanek KD, Murphy SL. Deaths: final data for 1997. Natl Vital Stat Rep 1999;47(19):101–4.
[2] Panos RJ, King TE. Idiopathic pulmonary fibrosis. In: Bone RC, editor. Pulmonary and critical care medicine. St. Louis: Mosby-Year Book Inc.; 1998. p. M3.
[3] Crouch E. Pathobiology of pulmonary fibrosis. Am J Physiol 1990;259(4 Pt 1): L159–84.
[4] Crystal RG, Ferrans VJ, Basset F. Biological basis of pulmonary fibrosis. In: Crystal RG, editor. The lung. New York: Raven Press; 1991. p. 2031.
[5] Mapel DW, Samet JM, Coultas DB. Corticosteroids and the treatment of idiopathic pulmonary fibrosis. Past, present, and future. Chest 1996;110(4):1058–67.
[6] Sivadas N, O'Rourke D, Tobin A, Buckley V, Ramtoola Z, Kelly JG, et al. A comparative study of a range of polymeric microspheres as potential carriers for the inhalation of proteins. Int J Pharm 2008;358(1):159–67.
[7] Xu FH, Zhang Q. Recent advances in the preparation progress of protein/peptide drug loaded PLA/PLGA microspheres. Yao Xue Xue Bao 2007;42(1):1–7.
[8] Cryan SA. Carrier-based strategies for targeting protein and peptide drugs to the lungs. AAPS J 2005;7(1):E20–41.
[9] Lombry C, Bosquillon C, Preat V, Vanbever R. Confocal imaging of rat lungs following intratracheal delivery of dry powders or solutions of fluorescent probes. J Control Release 2002;83(3):331–41.
[10] Sung JC, Pulliam BL, Edwards DA. Nanoparticles for drug delivery to the lungs. Trends Biotechnol 2007;25(12):563–70.
[11] Komada F, Iwakawa S, Yamamoto N, Sakakibara H, Okumura K. Intratracheal delivery of peptide and protein agents: absorption from solution and dry powder by rat lung. J Pharm Sci 1994;83(6):863–7.
[12] Springer C, Benita S, Sherman Y, Gursoy N, Gilhar D, Avital A. Poly-lactic-glycolic acid microspheres: a biodegradable marker for the diagnosis of aspiration in hamsters. Pediatr Res 2005;58(3):537–41.
[13] Houchin ML, Heppert K, Topp EM. Deamidation, acylation and proteolysis of a model peptide in PLGA films. J Control Release 2006;112(1): 111–9.
[14] Yang SC, Bhide M, Crispe IN, Pierce RH, Murthy N. Polyketal copolymers: a new acid-sensitive delivery vehicle for treating acute inflammatory diseases. Bioconjug Chem 2008;19(6):1164–9.

[15] Kinnula VL, Crapo JD. Superoxide dismutases in the lung and human lung diseases. Am J Respir Crit Care Med 2003;167(12):1600–19.
[16] Kinnula VL, Myllarniemi M. Oxidant-antioxidant imbalance as a potential contributor to the progression of human pulmonary fibrosis. Antioxid Redox Signal 2008;10(4):727–38.
[17] Bowler RP, Nicks M, Warnick K, Crapo JD. Role of extracellular superoxide dismutase in bleomycin-induced pulmonary fibrosis. Am J Physiol Lung Cell Mol Physiol 2002;282(4):L719–26.
[18] Fattman CL, Chang LY, Termin TA, Petersen L, Enghild JJ, Oury TD. Enhanced bleomycin-induced pulmonary damage in mice lacking extracellular superoxide dismutase. Free Radic Biol Med 2003;35(7):763–71.
[19] Fattman CL, Chu CT, Kulich SM, Enghild JJ, Oury TD. Altered expression of extracellular superoxide dismutase in mouse lung after bleomycin treatment. Free Radic Biol Med 2001;31(10):1198–207.
[20] Kinnula VL, Hodgson UA, Lakari EK, Tan RJ, Sormunen RT, Soini YM, et al. Extracellular superoxide dismutase has a highly specific localization in idiopathic pulmonary fibrosis/usual interstitial pneumonia. Histopathology 2006;49(1):66–74.
[21] Lakari E, Paakko P, Pietarinen-Runtti P, Kinnula VL. Manganese superoxide dismutase and catalase are coordinately expressed in the alveolar region in chronic interstitial pneumonias and granulomatous diseases of the lung. Am J Respir Crit Care Med 2000;161(2):615–21.
[22] Liu J, Wang X, Wang F, Teng L, Cao J. Attenuation effects of heparin-superoxide dismutase conjugate on bleomycin-induced lung fibrosis in vivo and radiation-induced inflammatory cytokine expression in vitro. Biomed Pharmacother 2009;63(7):484–91.
[23] Machtay M, Scherpereel A, Santiago J, Lee J, McDonough J, Kinniry P, et al. Systemic polyethylene glycol-modified (PEGylated) superoxide dismutase and catalase mixture attenuates radiation pulmonary fibrosis in the C57/bl6 mouse. Radiother Oncol 2006;81(2):196–205.
[24] Carpenter M, Epperly MW, Agarwal A, Nie S, Hricisak L, Niu Y, et al. Inhalation delivery of manganese superoxide dismutase-plasmid/liposomes protects the murine lung from irradiation damage. Gene Ther 2005;12(8):685–93.
[25] Heffernon MJ, Kasturi SP, Yang SC, Pulendran B, Murthy N. The stimulation of CD8 + T cells by dendritic cells pulsed with polyketal microparticles containing ion-paired protein antigen poly(inosinic acid)-poly(cytidylic acid). Biomaterials 2009;30(5):910–8.
[26] Morita T, Horikiri Y, Yamahara H, Suzuki T, Yoshino H. Formation and isolation of spherical fine protein microparticles through lyophilization of protein-poly(ethylene glycol) aqueous mixture. Pharm Res 2000;17(11):1367–73.
[27] Iyer SS, Ramirez AM, Ritzenthaler JD, Torres-Gonzalez E, Roser-Page S, Mora AL, et al. Oxidation of extracellular cysteine/cystine redox state in bleomycin-induced lung fibrosis. Am J Physiol Lung Cell Mol Physiol 2009;296(1):L37–45.
[28] Rojas M, Xu J, Woods CR, Mora AL, Spears W, Roman J, et al. Bone marrow-derived mesenchymal stem cells in repair of the injured lung. Am J Respir Cell Mol Biol 2005;33(2):145–52.
[29] Izbicki G, Or R, Christensen TG, Segel MJ, Fine A, Goldstein RH, et al. Bleomycin-induced lung fibrosis in IL-4-overexpressing and knockout mice. Am J Physiol 2002;283(5):L1110–6.
[30] Sjogren F, Groth O, Anderson C. Acetone has anti-inflammatory effects on experimental contact reactions. Contact Derm 1999;41(1):22–9.